3D-NCuts: Adapting Normalized Cuts to 3D Triangulated Surface Segmentation

Zahra Toony[1], Denis Laurendeau[1], Philippe Giguère[2] and Christian Gagné[1]
[1]*Computer Vision and System Laboratory, Department of Electrical and Computer Engineering, Université Laval, Québec, QC, Canada*
[2]*Department of Computer Science and Software Engineering, Université Laval, Québec, QC, Canada*
zahra.toony.1@ulaval.ca, denis.laurendeau@gel.ulaval.ca, philippe.giguere@ift.ulaval.ca, christian.gagne@gel.ulaval.ca

Keywords: 3D segmentation, spectral 3D segmentation, primitive extraction from mesh models, clustering.

Abstract: Being able to automatically segment 3D models into meaningful parts is an important goal in 3D shape processing. In this paper, we are proposing a fast and easy-to-implement 3D segmentation approach, which is based on spectral clustering. For this purpose, we define an improved formulation of the similarity matrix which allows our algorithm to segment both free-form and CAD (Computer Aided Design) 3D models. In 3D space, different shapes, such as planes and cylinders, have different surface normal distributions. We defined the similarity of vertices based on their normals which can segment a 3D model into its geometric features. Results show the effectiveness and robustness of our method in segmenting a wide range of 3D models. Even in the case of complex models, our method results in meaningful segmentations. We tested our segmentation approach on real data segmentation, in the presence of noise and also in comparison with other methods which provided good results in all cases.

1 INTRODUCTION

In the early 1980s, availability of precise 2D and 3D cameras has opened a new field of computer vision, 3D image acquisition and processing (Blais, 2004). Nowadays, this field has many different applications such as assembly, inspection, Computer-aided Design (CAD), reverse engineering, mechanical engineering, medicine, and entertainment.

Standard 2D cameras produce 2D images from the surface of objects, in either black-and-white or color, but 3D cameras provide information on the geometry of the object surface. Today, some 3D cameras can acquire both the appearance and geometry of objects concurrently. This results in many 2D processing approaches applied on 3D images: 3D mesh compression (Yu et al., 2012; Jiang et al., 2012; Carnero et al., 2012), 3D skeleton extraction (Sam et al., 2012; Zhang et al., 2012; Benhabiles et al., 2012), 3D object recognition (Karim Baareh et al., 2012; Huber et al., 2004; Murase and Nayar, 1995; Selinger and Nelson, 1999), and 3D segmentation (Xiao et al., 2011; Liu and Zhang, 2004; Lavoué et al., 2012) are instances of such extensions of 2D approaches to 3D.

One of the challenges in shape processing and understanding is to segment a 3D object into meaningful parts (Ning et al., 2010). This implies segmenting a 3D shape, not based on distances, but rather based on its properties to obtain a result close to a manual segmentation. Many applications, such as object recognition, modelling, or compression depend on meaningful segmentation (Kalogerakis et al., 2010). In some other applications, segmentation is used to label parts of the shapes; many of these approaches use manually segmented shapes. For example, in a human body one could distinguish "arm", "leg", and "head" from each other (Kalogerakis et al., 2010). Ground-truth databases for segmentation of 3D-meshes were created recently, (Benhabiles et al., 2009; Chen et al., 2009). They offer the opportunity of analyzing and learning mesh segmentation quantitatively (Benhabiles et al., 2011).

Based on what is presented in (Shamir, 2008), algorithms in 3D mesh segmentation can be categorized into five groups while the paper by (Agathos et al., 2007) presented a more detailed classification of 3D mesh segmentation methods into twelve groups: "Region growing", "Watershed-based", "Reeb graphs", "Model-based", "Skeleton-based", "Clustering", "Spectral analysis", "Explicit Boundary Extraction", "Critical points-based", "Multiscale Shape Descriptors", "Markov Random Fields" and "Direct segmentation". To find more details on methods in each category refer to (Shamir, 2008; Agathos et al., 2007). Each of these groups can perform the segmentation in two main ways: *surface-based* and *part-based*. A surface-based 3D mesh segmentation method attempts to segment a model into different regions under some criteria that can be estimated by simple shapes such as planes or cylinders. On the other hand, a part-based approach attempts to segment it into meaningful volumetric parts (Agathos et al., 2007).

In this work, we study the segmentation of a 3D model with a spectral analysis approach in a surface-based paradigm. Spectral analysis methods are based on a similarity matrix. Our focus here is to define a similarity matrix that avoids thresholding and works without using training data. We introduce two parameters in order to improve the quality of segmentation results. It can discriminate different parts with different geometries very well, thus resulting in meaningful mesh segmentation.

The rest of the paper is organized as follows. The related works are represented in Section 2. In Section 3, we explain our problem and present the details of our novel 3D Normalized Cuts approach. Section 4 shows the efficiency of our approach and gives the experimental results obtained in different situations and in comparison with other methods. Finally, we conclude the paper in Section 5.

2 RELATED WORK

Conducting a meaningful segmentation of a 3D model is generally application dependent. In our case, we call a segmentation *meaningful* when it can separate different geometries from each other as a human does. Among different types of mesh segmentation methods, spectral analysis has attracted much attention.

The theory of spectral graphs was introduced by (Chung, 1997) and was then applied on image segmentation by (Shi and Malik, 2000) as Normalized Cuts (NCuts). 3D spectral analysis approaches first define a similarity matrix on the data, based on properties of mesh connectivity, geometry, etc. Then, a Laplacian matrix is computed based on the defined similarity and its eigenvectors are determined in order to segment the 3D model. Since the Laplacian matrix and eigenvectors are found based on the similarity matrix, the most important step of the spectral analysis methods is how the similarity is defined such that good segmentations are then obtained.

In 2004, Liu and Zhang (Liu and Zhang, 2004) applied spectral analysis on 3D models. They defined the similarity matrix as the likelihood that faces belong to the same segment. In order to prevent merging faces with different concavities, they used the distance matrix presented in (Shlafman et al., 2002; Katz and Tal, 2003). They constructed the normalized similarity matrix on the faces and then identified the k eigenvectors with the largest associated eigenvalues for further processing. Finally, they applied k-means on the processed eigenvectors. They segmented a model by emphasizing concavities, which sometimes resulted in segmenting unmeaningful concavities (Agathos et al., 2007). Another method (Zhang and Liu, 2005) used the same similarity matrix with recursive spectral cut and Nyström approximation (Fowlkes et al., 2004), which gave them the opportunity of defining a partial similarity matrix. The extracted eigenvectors are then used in a line search algorithm to find the most prominent cut in order to segment the 3D model. In (Liu and Zhang, 2007), a spectral analysis algorithm based on spectral embedding and 2D contour analysis was proposed. The 3D model was projected into the 2D domain in order to apply contour analysis. The algorithm required that some parameters be selected, and tended to fail in the presence of noise.

Some other types of segmentation algorithms are based on region growth. In these methods, a seed point is first selected and then grown, in order to find final regions. This often leads to over-segmentation (Zhang et al., 2002). Watershed-based approaches are also subject to over-segmentation of the 3D models (Agathos et al., 2007).

Some other methods, such as Randomized Cuts (Golovinskiy and Funkhouser, 2008), take the advantages of using different segmentation methods to gain both random and non-random features. In order to segment a 3D model, Golovinskiy and Funkhouser (Golovinskiy and Funkhouser, 2008) generate a pool of segmented parts using different approaches such as k-means (Shlafman et al., 2002), hierarchical Normalized Cuts and Min Cuts. Afterwards, based on the reputation of each edge on a segmentation boundary, they define a "partition function" on edges. The "consistent cuts" are then found and the model is segmented through these cuts.

For the k-means approach, they set the number of clusters and repeat the k-means algorithm several times in order to generate different segmentation results. In the hierarchical Normalized Cuts method, they start with every face in a separate segment and then try to merge them based on an area-normalized cut cost function until the desired number of clusters is obtained. The cost function is the sum of the cut costs of segments divided by their areas. They are using this cost function, called modified version of Normalized Cuts, instead of using only the cost of all edges in a segment which is utilized as Normalized Cuts in (Shi and Malik, 2000). This algorithm is repeated to obtain different results. Finally, in the Min Cuts approach a set of k seeds is selected and a weight value is defined for each edge in order to maintain the cuts at a large distance from the seeds. This method is also repeated to provide more different segmentation results.

In (Lai et al., 2008) a random walk approach is utilized in order to achieve a mesh segmentation. The authors compute the dual graph of the mesh and select the seeds automatically; the numbers of seeds are greater than the desired number of clusters. They then try to associate each face with a seed with the highest probability which results in an over segmented mesh. Hence, a hierarchical method is then applied to merge the similar segments based on the length of common boundaries and overall perimeter of adjacent segments (Chen et al., 2009).

The hierarchical fitting primitive approach that is proposed in (Attene et al., 2006) considers each face as a segment and starts to merge them until the desired number of clusters is obtained. At each iteration, a primitive like plane, sphere and etc. is fitted on each pair of faces and then the best fitted pair will be merged as a segment (Chen et al., 2009).

Another approach which is called Shape Diameter Function (SDF) (Shapira et al., 2008) defines a scalar function for every face of the mesh and produces a 1-D histogram. Then, a Gaussian Mixure Model is applied on the histogram to fit k Gaussian functions on each face and determine the probability of assigning faces to each SDF cluster. Finally an alpha-expansion graph cut method is used to minimize a defined energy function in order to find the appropriate segmentation. This method determines the number of clusters automatically (Chen et al., 2009).

Recently, a mesh segmentation method for CAD models was presented in (Xiao et al., 2011). At first, the CAD model is clustered into sparse and dense triangle regions. Using the Gauss map of triangular faces and Hough transformation, sparse triangle regions are separated into planar regions, cylindrical regions and conical regions. Dense triangle regions are also segmented by a mean shift operation which is applied on the mean curvature field of mesh surfaces. One of the problems of this method is that it deals poorly with planar regions composed of non-uniform parts combining sparse and dense triangulations. This method will split the plane at first, without considering the geometry of the surface before splitting.

There are also some 3D segmentation methods based on learning algorithms (Kalogerakis et al., 2010; Benhabiles et al., 2011), which require a database of labeled meshes, a constraint that cannot be satisfied in many cases. Learning-based methods might achieve better segmentation results than other methods, however our approach does not use any training step or training data but rather considers the differences between geometries. As we aim at applying Normalized Cuts (Shi and Malik, 2000) in 3D space, the next sections explain the details of this method in 2D space.

2.1 2D-NCuts

Normalized Cuts (NCuts) (Shi and Malik, 2000) assumes that a 2D model is described as a graph $G = (V,E)$, where V is the set of vertices in our model and E is the set of edges (which transposes in 3D as a set of faces). The cut, or degree of dissimilarity between two segments, A and B, can be found by defining

$$cut(A,B) = \sum_{u \in A, v \in B} w(u,v), \tag{1}$$

where, $w(u,v)$ is the similarity between vertex u and v. Normalized Cuts aims at minimizing the $Ncut$ value

$$Ncut(A,B) = \frac{cut(A,B)}{assoc(A,V)} + \frac{cut(A,B)}{assoc(B,V)}, \tag{2}$$

where, $assoc(A,V) = \sum_{u \in A, t \in V} w(u,t)$ is the total similarity from all vertices in A to all vertices in the graph. This minimization is achieved by solving the following generalized eigenvalue system:

$$(\mathbf{D} - \mathbf{W})y = \lambda \mathbf{D} y, \tag{3}$$

where, $\mathbf{W}$ is the matrix of similarity between each pair of vertices and $\mathbf{D}$ is a diagonal matrix with:

$$d(i,i) = \sum_j w(i,j). \tag{4}$$

After solving Equation (3), the eigenvector related to the second smallest eigenvalue of the system is selected. It is claimed that this eigenvector keeps two vertices i and j in a segment when they have a large similarity value (large $w(i,j)$). The problem then consists in determining the splitting point of the eigenvector in such a way that the cut value between the two split parts is minimized. Shi and Malik presented an optimized loop for achieving this. Another way of splitting the eigenvector into different parts is applying a clustering method, such as k-means, to segment the vector into different regions.

3 PROPOSED IMPROVEMENTS TO NCUTS

Our goal is to separate a 3D model into meaningful parts. We desire to detect different parts based on different geometric primitives such as planes, cylinders, cubes, and rods. So, the differences between these geometric primitives must be described through a similarity matrix. In 3D space, it is clear that all vertices on a plane have normals in the same direction; all vertices on a cylinder have normals rotating uniformly on a circle, as can be seen in Figure 1b.

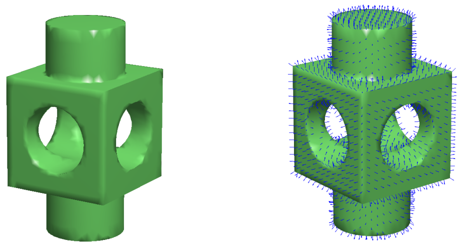

(a) (b)

Figure 1: (a) 3D model, (b) normals to the surface of 3D model.

Therefore we argue that defining the similarity based on normals is a good strategy to discriminate and to separate 3D geometric primitives. We thus define the similarity matrix as a relation between normal vectors that can reveal sharp edges and boundaries (see Figure 2). The similarity between two vertices is then defined as:

$$w(i,j) = \cos \prec (\vec{n}_i, \vec{n}_j), \tag{5}$$

where, $\vec{n}_i$ and $\vec{n}_j$ are normal vectors at vertices i and j, respectively. As shown in Figure 2, we observe large values of *w(i,j)* where surface normals are similar (red), but really small values at the boundaries between primitives (green) which can help us to separate different primitives. With this definition of similarity matrix, we then solve an eigenvalue system in order to find the segmentation results. This contrast the approach proposed in (Golovinskiy and Funkhouser, 2008), where they used the modified Normalized Cuts idea to find the cost function of a hierarchical clustering approach in order to merge faces. Here, we produce the segmentation on vertices which, with an accurate definition of normals, can else be applicable to point clouds.

The next sections present the details of our approach for 3D models.

Algorithm 1: Proposed 3D-NCuts

Input: similarity matrix $\mathbf{W}$, diagonal matrix $\mathbf{D}$ and number of clusters k.

1. Compute the similarity matrix $\mathbf{W}$,

$$w(i,j) = \begin{cases} \cos \prec (\vec{n}_i, \vec{n}_j) & \text{if } i \text{ and } j \text{ are connected by an edge} \\ 0 & \text{otherwise} \end{cases}$$

2. Evaluate the diagonal matrix $\mathbf{D}$, $d(i,i) = \sum_j w(i,j)$.
3. Solve the following generalized eigensystem, $(\mathbf{D}-\mathbf{W})y = \lambda \mathbf{D} y$.
4. Suppose V_{eig} as a matrix of the k eigenvectors associated with the k smallest eigenvalues.
5. Apply a clustering method, such as k-means, on V_{eig} to achieve k segments.

Output: Clusters $C_1, C_2, \ldots, C_k$.

3.1 Our approach: 3D-NCuts

As mentioned in Section 2.1 the Normalized Cuts algorithm begins by defining a similarity matrix on 3D data. Here we applied this method on 3D shapes and brought some modifications to the basic algorithm as presented in Algorithm 1.

Figure 3b presents the result of applying 3D-NCuts on a 3D model in order to segment the model into four clusters. It is observed that the result is not meaningful, especially on the handle of the mug; to circumvent this problem, we apply an exponential function on the weights of similarity to make small weight values even smaller and large values larger. This modification separates regions very well but, in order to assign a priority to the neighbours in comparison with the points that are far from each other, a small value η is added to the weights of neighbouring vertices. This parameter (η) forces the algorithm to always consider neighboring surfaces to be candidate for merger. Therefore the similarity matrix is rede-

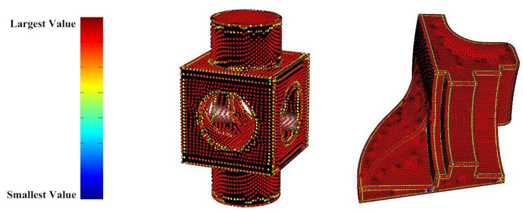

Figure 2: A color-coded representation of the similarity matrix values for two 3D models, where, blue indicates the lowest value and red indicates the largest value.

fined as

$$w(i,j) = \begin{cases} e^{\alpha \cos \sphericalangle(\vec{n}_i, \vec{n}_j)} + \eta & \text{if } i \text{ and } j \text{ are connected by an edge} \\ 0 & \text{otherwise} \end{cases} \tag{6}$$

As represented in Figure 3c, the modified similarity matrix renders the segmentation meaningful. When a human wishes to segment this 3D model into four segments it separates it into the handle, the bottom, the inner part of the mug and the outer part of the mug. This is precisely what the 3D-NCuts algorithm does to achieve the mug model. Henceforth, Equation 6 is used in the first step of Algorithm 1 and results in a better segmentation for all other 3D models.

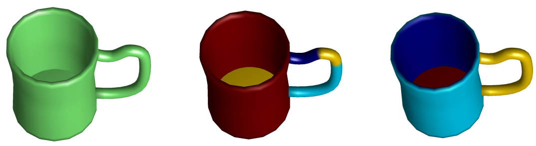

(a) (b) (c)

Figure 3: (a) 3D model, (b) result of 3D-NCuts segmentation with $k = 4$ and using the similarity matrix presented in step 1 of Algorithm 1. (c) result of 3D-NCuts segmentation with the modified weight Equation 6, with $k = 4$, $\alpha = 15$, $\eta = 0.5$ (after replacing the similarity equation in step 1 of Algorithm 1 by Equation 6).

The experimental results of 3D segmentation are presented in the next section, which shows the good performance of our approach.

4 Experimental results

We tested the performance of our approach on various 3D shapes, for different conditions and in comparison with other methods. We evaluated this method on objects we scanned with a handheld scanner (i.e., Creaform Go!SCAN handheld 3D scanner) as well as on 3D models with artificial noise.

The free-form 3D models that are used in the experiments and the results of segmentation by the approaches presented in Figure 5 are taken from the Princeton Shape Benchmark for 3D Segmentation (Chen et al., 2009). The 3D CAD models are taken from the database of Purdue University (ESB) (Jayanti et al., 2006).

The values of similarities between vertices (Equation 5) are between -1 and 1. For parameter α in $e^{\alpha w(i,j)}$, choosing a too small value does not create a large difference between weights on the boundaries and the ones on the surface. Choosing a large value also weakens some useful weights near the high weights. Since we desire to have a large difference between the weights on the surface and those on the boundaries, in all experiments, α is set to an intermediary value of $\alpha = 15$. The value of η specifies the impact of neighbour vertices which is set to 0.5 to keep both dependency and independency of a vertex to the neighbouring vertices.

Figure 5 shows the segmentation results using our method in comparison with some recent approaches. In this figure, we presented the segmentation results for four different 3D models. In each row, column (a) shows the result of our 3D-NCuts segmentation, column (b) presents manual segmentation which is the ground truth of presented 3D models. Columns (c), (d), (e), (f), and (g) represent the segmentation results using Randomized Cuts (Golovinskiy and Funkhouser, 2008), Normalized Cuts presented in (Golovinskiy and Funkhouser, 2008), Random walk (Lai et al., 2008), fitting primitive (Attene et al., 2006) and shape diameter (Shapira et al., 2008) approaches, respectively. The results show that in comparison to other methods, our segmentation approach is able to provide a 3D segmented model which more clearly resembles the ground truth.

Figure 6 shows some results of our method for CAD models in comparison with a recently presented CAD model segmentation method (Xiao et al., 2011). This approach segments the model automatically without considering the number of clusters. The results of the method proposed by (Xiao et al., 2011) in Figure 6, are obtained from their prepared GUI. Since their method is based on Hough transform and Gauss sphere mapping to detect planes and cylinders, it can detect these primitives very well but it sometimes fails to associate the parts together (such as the red line, in Figure 6, in the last column of the first row, on cylinder at the bottom part of the object which is detected as the top cylinder).

As shown in Figure 6, our method can segment a 3D CAD model very well. The segmentation results are presented with different number of clusters to show the effectiveness of our method in detecting more geometric primitives. In the first row, where the object was segmented into three clusters, our method separated the cylinder from the cube-like shape: the planes of the cube which are located in the same direction as those of the cylinder have been included with the cylinder, separating them from the remainder of the cube-like shape. In the case of $k = 8$, it also detects the cylinder, planes and four sides of the cube-like shape. In the second row, the results of segmenting the "fandisk" model into three and eight clusters, show that our method achieves better results than the method presented in (Xiao et al., 2011). With an increasing number of clusters our approach detects

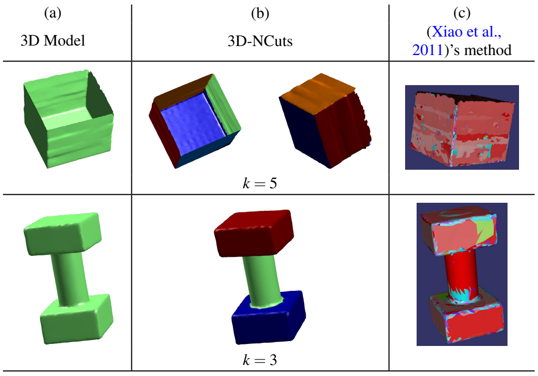

Figure 4: The result of our 3D segmentation approach in comparison with the method proposed by (Xiao et al., 2011) on real scanned data. 3D models are presented in column (a); column (b) and (c) show the result of segmentation by 3D-NCuts and the method presented in (Xiao et al., 2011), respectively.

more different geometric primitives as well.

In Figure 4, we present the segmentation results for real 3D data. We scanned two real objects in our lab to evaluate the efficiency of our method on real data. The models were scanned with an accuracy of 2 mm with the Go!SCAN scanner. As observed, our method segments the real CAD models much better than the approach presented in (Xiao et al., 2011) for CAD models. This illustrates that the method presented in (Xiao et al., 2011) is not robust in the presence of noise, even at low levels.

To further demonstrate the robustness of our algorithm in the presence of noise, we added some Gaussian noise to both free-form and CAD mesh models and applied our approach to segment these shapes. These models, with this small amount of vertices, are sensitive even in the presence of small noise levels. Figure 7 shows the segmentation results in the case of noiseless and noisy models. Column (c) of Figure 7 shows the segmentation results obtained using 3D-NCuts. Considering noisy and pure models, the results of segmenting a 3D model are almost the same with or without noise. For the mug model shown in second column, the 3D-NCuts algorithm segments the noisy mug into virtually the same four clusters as is the case for the noiseless mug. These results indicate that our approach is relatively stable, even in the presence of noise. To further illustrate the effectiveness of our approach more results of segmentation are presented in Figure 8. As can be observed, our methods are applicable for both 3D free-form and CAD models. For example, for the horse model with 10 clusters, 3D-NCuts segments the shape into four different segments of legs, two segments of ears and one segment for each of the following: tail, eyes, face and body. Different meaningful geometric features of the other models in this figure are obtained as well.

5 CONCLUSIONS

In this paper, we presented a spectral-based 3D segmentation method. This method, 3D-NCuts, identifies the Laplacian matrix of the 3D data and attempts to solve the segmentation problem based on the idea of 2D Normalized Cuts. The most important part of this method is the definition of the similarity matrix. Here, we defined this matrix based on normals of vertices and applied an exponential function with considering some constants to discriminate different geometries from each other in an object. The results show the efficiency of this approach for both free-form and CAD 3D models in comparison with other methods. The results are very similar to manual segmentation (the ground truth) which reveals our approach is able to produce meaningful segmentation. From the results, our method works better or at least similarly to other presented methods. We also tested our approach on real scanned data with good results. Even in the presence of significant noise, our approach was able to produce significant segmentation.

ACKNOWLEDGEMENTS

This work was supported by the NSERC-Creaform Industrial Research Chair on 3D Sensing. Z. Toony was supported by a FRQ-NT post-graduate scholarship. The authors thank Hongwei Lin for providing us with the GUI of their method (Xiao et al., 2011).

REFERENCES

Agathos, A., Pratikakis, I., Perantonis, S., Sapidis, N., and Azariadis, P. (2007). 3D mesh segmentation methodologies for CAD applications. *Computer-Aided Design and Applications*, 4(6):827–841.

Attene, M., Falcidieno, B., and Spagnuolo, M. (2006). Hierarchical mesh segmentation based on fitting primitives. *The Visual Computer*, 22(3):181–193.

Benhabiles, H., Lavoué, G., Vandeborre, J.-P., and Daoudi, M. (2011). Learning boundary edges for 3D-Mesh segmentation. In *Computer Graphics Forum*, volume 30, pages 2170–2182. Wiley Online Library.

Benhabiles, H., Lavoué, G., Vandeborre, J.-P., Daoudi, M., et al. (2012). Kinematic skeleton extraction based on motion boundaries for 3D dynamic meshes. In *Eurographics 2012 Workshop on 3D Object Retrieval*, pages 71–76.

Benhabiles, H., Vandeborre, J.-P., Lavoué, G., and Daoudi, M. (2009). A framework for the objective evaluation of segmentation algorithms using a ground-truth of human segmented 3D-models. In *IEEE International Conf. on Shape Modeling and Applications (SMI)*, pages 36–43.

Blais, F. (2004). Review of 20 years of range sensor development. volume 13, pages 231–243. Journal of Electronic Imaging.

Carnero, J., Molina-Abril, H., and Real, P. (2012). Triangle mesh compression and homological spanning forests. In *Proceedings of the 4th international conf. on Computational Topology in Image Context*, pages 108–116.

Chen, X., Golovinskiy, A., and Funkhouser, T. (2009). A benchmark for 3D mesh segmentation. *ACM Transactions on Graphics (TOG)*, 28(3):73.

Chung, F. R. (1997). Spectral graph theory. *CBMS Regional Conference Series in Mathematics*, 92.

Fowlkes, C., Belongie, S., Chung, F., and Malik, J. (2004). Spectral grouping using the Nystrom method. *IEEE Transactions on Pattern Analysis and Machine Intelligence*, 26(2):214–225.

Golovinskiy, A. and Funkhouser, T. (2008). Randomized cuts for 3D mesh analysis. In *ACM Transactions on Graphics (TOG)*, volume 27, page 145.

Huber, D., Kapuria, A., Donamukkala, R., and Hebert, M. (2004). Parts-based 3D object classification. In *Computer Vision and Pattern Recognition (CVPR)*, volume 2, pages 82–89.

Jayanti, S., Kalyanaraman, Y., Iyer, N., and Ramani, K. (2006). Developing an engineering shape benchmark for CAD models. *Computer-Aided Design*, 38(9):939–953.

Jiang, W., Tian, J., Cai, K., Zhang, F., and Luo, T. (2012). Tangent-plane-continuity maximization based 3D point compression. In *19th IEEE International Conf. on Image Processing (ICIP)*, pages 1277–1280.

Kalogerakis, E., Hertzmann, A., and Singh, K. (2010). Learning 3D mesh segmentation and labeling. *ACM Transactions on Graphics (TOG)*, 29(4):102.

Karim Baareh, A., Sheta, A. F., and Al-Batah, M. S. (2012). Feature based 3D object recognition using artificial neural networks. *International Journal of Computer Applications*, 44(5):1–7.

Katz, S. and Tal, A. (2003). *Hierarchical mesh decomposition using fuzzy clustering and cuts*, volume 22. ACM Trans. on Graphics.

Lai, Y.-K., Hu, S.-M., Martin, R. R., and Rosin, P. L. (2008). Fast mesh segmentation using random walks. In *Proceedings of the ACM symposium on Solid and physical modeling*, pages 183–191.

Lavoué, G., Vandeborre, J.-P., Benhabiles, H., Daoudi, M., Huebner, K., Mortara, M., Spagnuolo, M., et al. (2012). SHREC'12 Track: 3D mesh segmentation. In *Eurographics 2012 Workshop on 3D Object Retrieval*, pages 93–99.

Liu, R. and Zhang, H. (2004). Segmentation of 3D meshes through spectral clustering. In *Proceedings. 12th Pacific Conf. on Computer Graphics and Applications*, pages 298–305.

Liu, R. and Zhang, H. (2007). Mesh segmentation via spectral embedding and contour analysis. In *Computer Graphics Forum*, volume 26, pages 385–394. Wiley Online Library.

Murase, H. and Nayar, S. K. (1995). Visual learning and recognition of 3-D objects from appearance. *International journal of computer vision*, 14(1):5–24.

Ning, X., Li, E., Zhang, X., and Wang, Y. (2010). Shape decomposition and understanding of point cloud objects based on perceptual information. In *Proceedings of the 9th ACM SIGGRAPH Conf. on Virtual-Reality Continuum and its Applications in Industry*, pages 199–206.

Sam, V., Kawata, H., and Kanai, T. (2012). A robust and centered curve skeleton extraction from 3D point cloud. *Computer-Aided Design & Applications*, 9(6):869–879.

Selinger, A. and Nelson, R. C. (1999). A perceptual grouping hierarchy for appearance-based 3D object recognition. *Computer Vision and Image Understanding*, 76(1):83–92.

Shamir, A. (2008). A survey on mesh segmentation techniques. In *Computer graphics forum*, volume 27, pages 1539–1556. Wiley Online Library.

Shapira, L., Shamir, A., and Cohen-Or, D. (2008). Consistent mesh partitioning and skeletonisation using the shape diameter function. *The Visual Computer*, 24(4):249–259.

Shi, J. and Malik, J. (2000). Normalized cuts and image segmentation. *IEEE Transactions on Pattern Analysis and Machine Intelligence*, 22(8):888–905.

Shlafman, S., Tal, A., and Katz, S. (2002). Metamorphosis of polyhedral surfaces using decomposition. In *Computer Graphics Forum*, volume 21, pages 219–228. Wiley Online Library.

Xiao, D., Lin, H., Xian, C., and Gao, S. (2011). CAD mesh model segmentation by clustering. *Computers & Graphics*, 35(3):685–691.

Yu, H., Chen, J., Wan, W., Wang, R., and Yu, X. (2012). A segmentation progressive mesh compression method. In *International Conf. on Audio, Language and Image Processing (ICALIP)*, pages 1163–1166.

Zhang, H. and Liu, R. (2005). Mesh segmentation via recursive and visually salient spectral cuts. In *Proc. of vision, modeling, and visualization*, pages 429–436.

Zhang, Q., Song, X., Shao, X., Shibasaki, R., and Zhao, H. (2012). Unsupervised skeleton extraction and motion capture from 3D point cloud sequences. *Neurocomputing*, 100.

Zhang, Y., Paik, J., Koschan, A., Abidi, M. A., and Gorsich, D. (2002). Simple and efficient algorithm for part decomposition of 3-D triangulated models based on curvature analysis. In *International Conference on Image Processing*, volume 3, pages III–273.

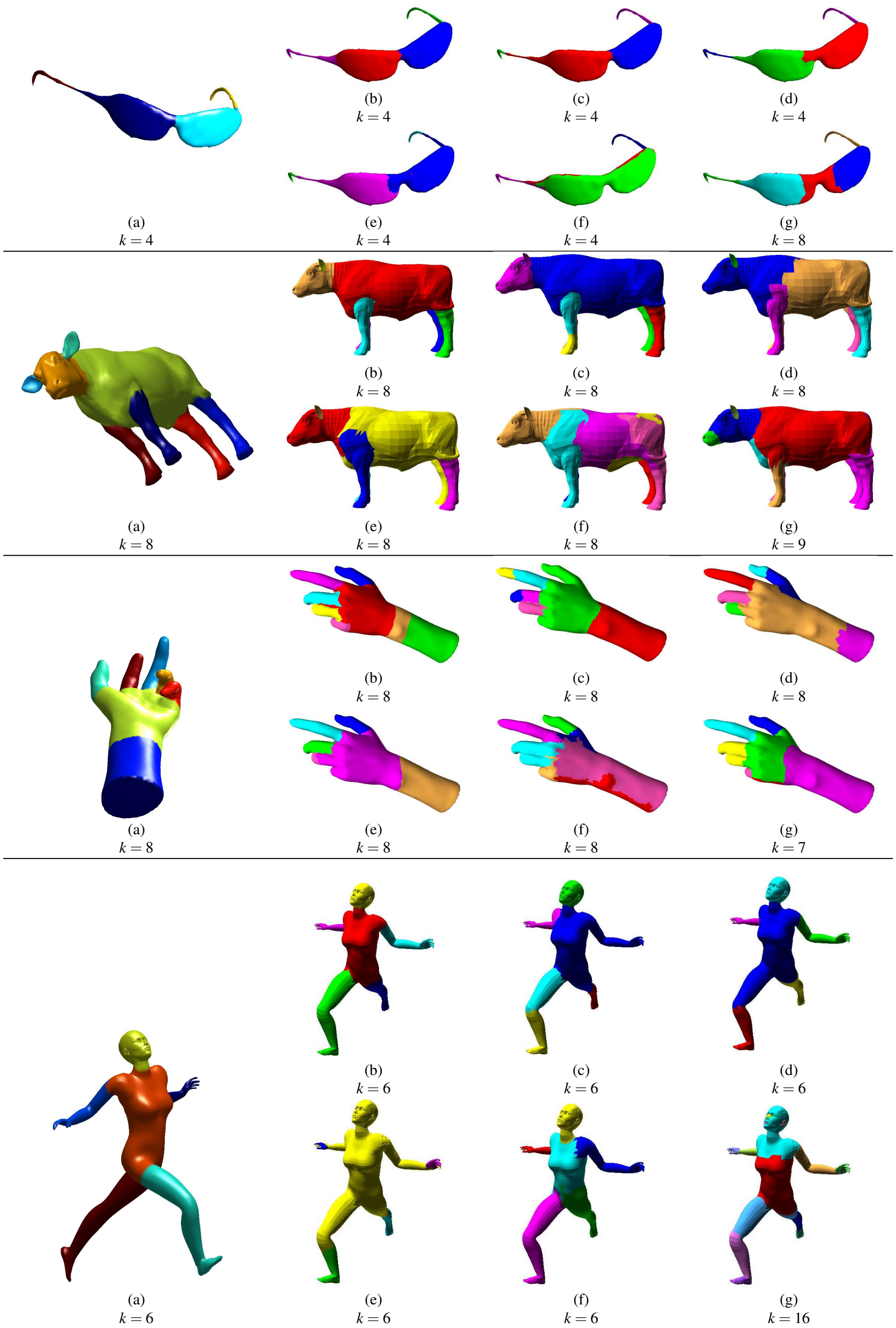

Figure 5: Comparison to previous segmentation methods. The methods that are compared (a) Our method, (b) Manual segmentation, (c) Randomized Cuts (Golovinskiy and Funkhouser, 2008), (d) Normalized Cuts presented in (Golovinskiy and Funkhouser, 2008), (e) Random Walk (Lai et al., 2008), (f) Fitting primitives (Attene et al., 2006), (g) Shape Diameter (Shapira et al., 2008). The last method, Shape Diameter (Shapira et al., 2008), is an automatic algorithm which determines the numbers of clusters.

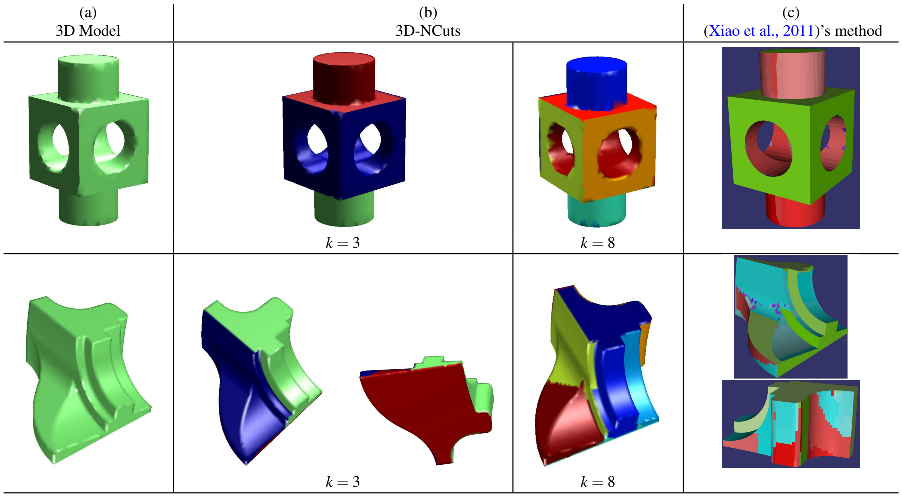

Figure 6: The result of our 3D segmentation method in comparison with the method proposed by (Xiao et al., 2011). Column (a) shows the 3D models, column (b) and (c) present the result of segmentation by 3D-NCuts and the method proposed by (Xiao et al., 2011), respectively. In the first row, column (b) shows results for different numbers of clusters.

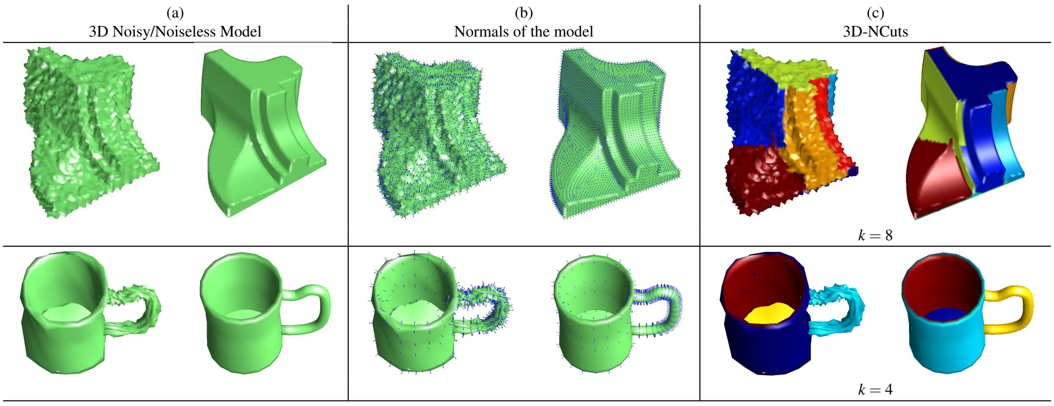

Figure 7: The result of our 3D segmentation approaches in the presence of noise. Column (a) shows the 3D noisy or noiseless models. The normals of models presented in column (a) are shown in column (b). Column (c) is representing the results of segmentation by 3D-NCuts for both noisy and noiseless models.

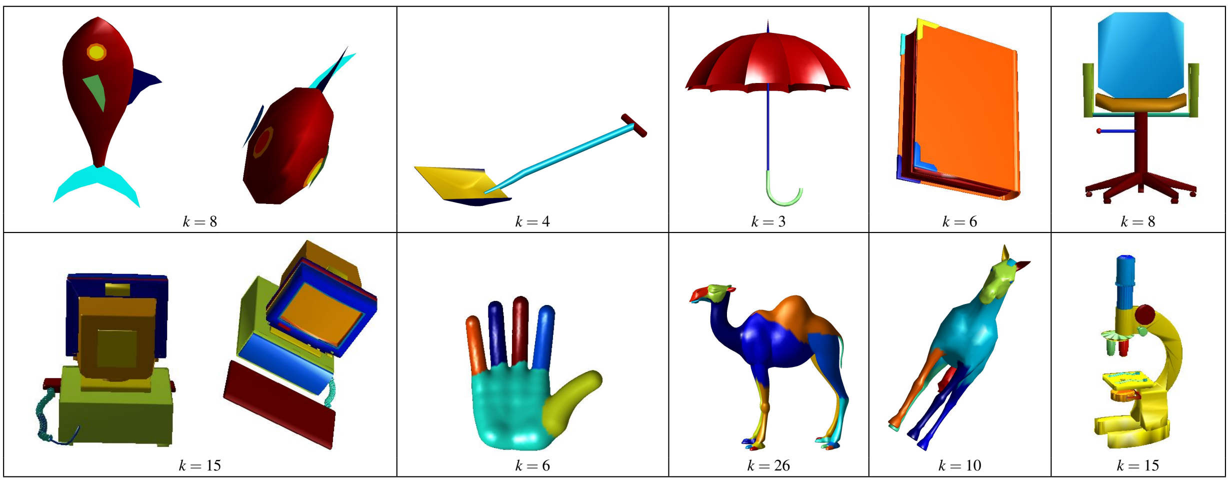

Figure 8: More results on our 3D segmentation approach.